ORIGINAL PAPER

Multiple system atrophy prions retain strain specificity after serial propagation in two different Tg(*SNCA**A53T) mouse lines

Amanda L. Woerman[1,2] · Abby Oehler[1] · Sabeen A. Kazmi[1] · Jisoo Lee[1] · Glenda M. Halliday[3,4,5] ·
Lefkos T. Middleton[6] · Steve M. Gentleman[7] · Daniel A. Mordes[8] · Salvatore Spina[2] · Lea T. Grinberg[2] ·
Steven H. Olson[1,2] · Stanley B. Prusiner[1,2,9]

Abstract

Previously, we reported that intracranial inoculation of brain homogenate from multiple system atrophy (MSA) patient samples produces neurological disease in the transgenic (Tg) mouse model TgM83$^{+/-}$, which uses the prion protein promoter to express human α-synuclein harboring the A53T mutation found in familial Parkinson's disease (PD). In our studies, we inoculated MSA and control patient samples into Tg mice constructed using a P1 artificial chromosome to express wild-type (WT), A30P, and A53T human α-synuclein on a mouse α-synuclein knockout background [Tg(*SNCA*$^{+/+}$)Nbm, Tg(*SNCA**A30P$^{+/+}$)Nbm, and Tg(*SNCA**A53T$^{+/+}$)Nbm]. In contrast to studies using TgM83$^{+/-}$ mice, motor deficits were not observed by 330–400 days in any of the Tg(*SNCA*)Nbm mice after inoculation with MSA brain homogenates. However, using a cell-based bioassay to measure α-synuclein prions, we found brain homogenates from Tg(*SNCA**A53T$^{+/+}$) Nbm mice inoculated with MSA patient samples contained α-synuclein prions, whereas control mice did not. Moreover, these α-synuclein aggregates retained the biological and biochemical characteristics of the α-synuclein prions in MSA patient samples. Intriguingly, Tg(*SNCA**A53T$^{+/+}$)Nbm mice developed α-synuclein pathology in neurons and astrocytes throughout the limbic system. This finding is in contrast to MSA-inoculated TgM83$^{+/-}$ mice, which develop exclusively neuronal α-synuclein aggregates in the hindbrain that cause motor deficits with advanced disease. In a crossover experiment, we inoculated TgM83$^{+/-}$ mice with brain homogenate from two MSA patient samples or one control sample first inoculated, or passaged, in Tg(*SNCA**A53T$^{+/+}$)Nbm animals. Additionally, we performed the reverse experiment by inoculating Tg(*SNCA**A53T$^{+/+}$)Nbm mice with brain homogenate from the same two MSA samples and one control sample first passaged in TgM83$^{+/-}$ animals. The TgM83$^{+/-}$ mice inoculated with mouse-passaged MSA developed motor dysfunction and α-synuclein prions, whereas the mouse-passaged control sample had no effect. Similarly, the mouse-passaged MSA samples induced α-synuclein prion formation in Tg(*SNCA**A53T$^{+/+}$)Nbm mice, but the mouse-passaged control sample did not. The confirmed transmission of α-synuclein prions to a second synucleinopathy model and the ability to propagate prions between two distinct mouse lines while retaining strain-specific properties provides compelling evidence that MSA is a prion disease.

Introduction

Multiple system atrophy (MSA) is a sporadic neurodegenerative disorder characterized by progressive autonomic and motor dysfunction. The term MSA was introduced in 1969 after Graham and Oppenheimer compared brain tissue from patients with olivopontocerebellar atrophy (OPCA), Shy–Drager syndrome (SDS), and striatonigral degeneration (SND), and concluded the three disorders were distinct clinical presentations of the same neuropathogenic process [8]. The subsequent identification of Papp–Lantos bodies, or

✉ Amanda L. Woerman
amanda.woerman@ucsf.edu

Extended author information available on the last page of the article

glial cytoplasmic inclusions (GCIs), in oligodendrocytes of OPCA, SDS, and SND patients supported this reclassification [28]. In 1998, two independent groups showed that the protein α-synuclein, which was linked to Parkinson's disease (PD) 1 year prior, aggregated to form GCIs in brain sections from deceased MSA patients [37, 39].

In the 20 years that followed this discovery, substantial work focused on developing transgenic (Tg) mouse models of α-synuclein misfolding and accumulation to better understand disease etiology and progression in the synucleinopathies, including PD and MSA. Mouse models overexpressing either wild-type (WT) or mutant human α-synuclein (*SNCA*) were created using central nervous system (CNS)–specific promoters to localize α-synuclein expression either in neurons to model PD [4–7, 11, 13, 18, 21, 23, 33, 35, 38, 46] or in oligodendrocytes to model MSA [14, 36, 44]. In the oligodendrocyte-specific models, spontaneous accumulation of α-synuclein was used to investigate neuroinflammation, demyelination, loss of dopaminergic neurons, and motor dysfunction in disease progression. These models were also used to identify and evaluate a vaccine to treat MSA in pre-clinical testing [22]. However, it remains unknown if the conformation of misfolded α-synuclein that develops in these mice is consistent with the conformation present in an MSA patient. Without this critical bridge, drug candidates may fail in clinical trials with MSA patients.

To meet this challenge, several studies have recently shown that brain homogenates from deceased MSA patient samples transmit neurological disease ~120 days post-inoculation (dpi) into the hemizygous TgM83$^{+/-}$ mouse model [31, 40–43]. TgM83$^{+/-}$ mice, which use the mouse prion protein promoter to express human α-synuclein with the A53T mutation [5], do not develop spontaneous disease [40]. However, inoculating these animals with MSA patient samples induces the accumulation of neuronal α-synuclein aggregates that are insoluble and hyperphosphorylated [31, 40]. Testing the biological and biochemical properties of the α-synuclein aggregates that develop in TgM83$^{+/-}$ mice showed that the resulting inclusions retain key characteristics of α-synuclein aggregates isolated from human MSA patient samples [41]. These findings argue that in MSA, α-synuclein misfolds into a self-templating conformation and becomes a prion.

In addition to the TgM83$^{+/-}$ mouse model, we report here attempts to transmit MSA to three Tg mouse models that express WT [Tg(*SNCA*$^{+/+}$)Nbm] or mutant α-synuclein [Tg(*SNCA**A30P$^{+/+}$)Nbm and Tg(*SNCA**A53T$^{+/+}$)Nbm]. The three Tg(*SNCA*)Nbm models were created using a P1 artificial chromosome, resulting in more widespread transgene expression, with the mouse α-synuclein gene knocked out [17]. Following inoculation with MSA patient samples, α-synuclein prions were only detected in asymptomatic Tg(*SNCA**A53T$^{+/+}$)Nbm mice terminated 330 dpi.

Similar to our previous observations with TgM83$^{+/-}$ mice, these aggregates retained biological and biochemical properties of α-synuclein prions isolated from MSA patient samples, demonstrating Tg(*SNCA**A53T$^{+/+}$)Nbm mice also propagate MSA prions with high fidelity. Notably, α-synuclein pathology in these animals accumulates in neurons and astrocytes throughout the limbic system in contrast to the exclusively neuronal hindbrain aggregates that contribute to autonomic and motor symptoms in TgM83$^{+/-}$ mice.

In serial passaging studies, brain homogenates from Tg(*SNCA**A53T$^{+/+}$)Nbm mice inoculated with two MSA patient samples induced neurological disease in TgM83$^{+/-}$ animals. While serially passaging the control patient sample had no effect in the mice, the passaged MSA samples caused neuronal α-synuclein inclusions to form throughout the hindbrain. In the reverse experiment, brain homogenates from TgM83$^{+/-}$ mice inoculated with the same MSA patient samples induced α-synuclein prion propagation in Tg(*SNCA**A53T$^{+/+}$)Nbm mice. These animals developed α-synuclein inclusions in the limbic system, whereas passaging studies with the control patient sample had no effect. Importantly, α-synuclein prions isolated from both mouse models showed similar biological activities and biochemical stabilities to α-synuclein prions isolated from MSA patient samples. These studies demonstrate that α-synuclein prions not only can propagate in two different Tg mouse models but also can be passaged from one model into the other while retaining MSA-specific strain characteristics. Our studies reported here extend earlier findings arguing that α-synuclein prions cause MSA.

Materials and methods

Human tissue samples

Frozen brain tissue samples from neuropathologically confirmed cases of MSA and PD were provided by the Sydney Brain Bank, the Parkinson's UK Tissue Bank at Imperial College, and the Massachusetts Alzheimer's Disease Research Center. Fixed and frozen brain tissue from two neuropathologically confirmed cases of MSA were provided by the Neurodegenerative Disease Brain Bank at the University of California, San Francisco. Control patient tissue was provided by Dr. Martin Ingelsson (Uppsala University) and Dr. Deborah Mash (Miami Brain Bank). Demographic information about samples used is included in Online Resource, Table S1.

Mice

Animals were maintained in an AAALAC-accredited facility in compliance with the *Guide for the Care and Use of Laboratory Animals*. All procedures used in this study were approved by the University of California, San Francisco, Institutional Animal Care and Use Committee. All animals were maintained under standard environmental conditions with a 12:12-h light:dark cycle and free access to food and water. The dbl-PAC-Tg($SNCA^{WT}$)$^{+/+}$;$Snca^{-/-}$, dbl-PAC-Tg($SNCA^{A30P}$)$^{+/+}$;$Snca^{-/-}$, and dbl-PAC-Tg($SNCA^{A53T}$)$^{+/+}$; $Snca^{-/-}$ [referred to here as Tg($SNCA^{+/+}$)Nbm, Tg($SNCA*$A30P$^{+/+}$)Nbm, and Tg($SNCA*$A53T$^{+/+}$)Nbm, respectively] were provided by Robert L. Nussbaum. To improve litter viability, all Tg($SNCA$)Nbm mouse pups used in these studies were fostered using CD-1 females purchased from The Jackson Laboratory (USA). TgM83$^{+/-}$ mice were generated by breeding TgM83$^{+/+}$ mice [5], purchased from The Jackson Laboratory, with B6C3F1 mice.

Inoculations

Fresh frozen human tissue and frozen mouse half-brains were used to create a 10% (wt/vol) homogenate using calcium- and magnesium-free 1× Dulbecco's phosphate-buffered saline (DPBS) using the Omni Tissue Homogenizer (Omni International). Homogenates were diluted to 1% using 5% (wt/vol) bovine serum albumin in 1× DPBS.

Eight-week-old Tg($SNCA^{+/+}$)Nbm, Tg($SNCA*$A30P$^{+/+}$) Nbm, and Tg($SNCA*$A53T$^{+/+}$)Nbm mice were anesthetized with isoflurane prior to inoculation. Free-hand inoculations with human patient samples were performed using 30 µL of the 1% brain homogenate into the thalamus. Following inoculation, all mice were assessed twice a week for the onset of neurological signs based on standard diagnostic criteria for prion disease [2]. Uninoculated Tg($SNCA^{+/+}$)Nbm mice were euthanized at 500 days of age. Uninoculated Tg($SNCA*$A30P$^{+/+}$)Nbm mice were euthanized between 450 and 500 days of age. Uninoculated Tg($SNCA*$A53T$^{+/+}$)Nbm mice were euthanized between 450 and 625 days of age. MSA-inoculated Tg($SNCA^{+/+}$) Nbm mice were euthanized 400 dpi, and Tg($SNCA*$A30P$^{+/+}$) Nbm and Tg($SNCA*$A53T$^{+/+}$)Nbm mice were collected 330 dpi. Tg($SNCA*$A53T$^{+/+}$)Nbm mice inoculated with brain homogenate from either control or MSA patient samples passaged in TgM83$^{+/-}$ mice were euthanized 300 dpi. Ten-week-old TgM83$^{+/-}$ mice inoculated with brain homogenate from MSA patient samples passaged through Tg($SNCA*$A53T$^{+/+}$) Nbm mice were euthanized after developing progressive neurological signs, or 450 dpi. Additionally, mice inoculated with brain homogenate from a control patient passaged in Tg($SNCA*$A53T$^{+/+}$)Nbm mice were euthanized 450 dpi. Following euthanasia, the brain was removed and bisected down the midline. The left hemisphere was frozen for biochemical analysis, and the right hemisphere was fixed in formalin for neuropathological assessment.

Alpha-synuclein prion quantification assay

A 10% (wt/vol) brain homogenate was prepared using frozen human tissue in calcium- and magnesium-free 1× DPBS using the Omni Tissue Homogenizer with disposable soft tissue tips (Omni International). Aggregated protein was isolated from the patient samples using sodium phosphotungstic acid (PTA; Sigma) as described [34, 43]. Isolated protein pellets were diluted 1:10 in 1× DPBS before testing in the α-synuclein prion quantification assays.

HEK293T cells expressing α-syn140–YFP, α-syn140* E46K–YFP, α-syn140*A53T–YFP, α-syn140*A30P,A53T– YFP, α-syn140*E46K,A53T–YFP, α-syn95*A53T–YFP, and α-syn97*A53T–YFP were previously reported, and culture and assay conditions were used as described [41]. Images of cells incubated with Tg mouse samples were collected using the IN Cell Analyzer 6000 (GE Healthcare). DAPI and FITC channels were used to collect two images from five different regions in each well. Each set of images was analyzed using the IN Cell Developer software with an algorithm created to detect intracellular aggregates in living cells, quantified as total fluorescence per cell ($\times 10^3$, arbitrary units, A.U.).

Immunohistochemistry and neuropathology

Mouse brains were fixed in 10% (vol/vol) formalin and cut into four sections prior to processing through graded alcohols, clearing with xylene, infiltrating with paraffin, and embedding. Thin slices (8 µm) were cut, collected on slides, deparaffinized, and exposed to heat-mediated antigen retrieval with citrate buffer (0.1 M, pH 6) for 20 min. Slides were stained using a Thermo Fisher 480S Autostainer with 30 min blocking in 10% (vol/vol) normal goat serum and incubation with primary antibody (2 h) and secondary antibody (2 h). Primary antibodies used include EP1536Y (pS129 α-synuclein; 1:1000; Abcam), MABN826 (pS129 α-synuclein; 1:250; Millipore), glial fibrillary acidic protein (GFAP; 1:500; Abcam), ionized calcium binding adaptor molecule 1 (Iba1; 1:250; Synaptic Systems), microtubule associated protein 2 (MAP2; 1:500; Abcam), and oligodendrocyte transcription factor 2 (Olig2; 1:500; Millipore). Secondary antibodies conjugated to AlexaFluor 488, 568, or 647 (Thermo Fisher) were used. Staining for co-localization of α-synuclein with neural/glial antigen 2 (NG2)–positive cells was done overnight at room temperature using MABN826 (pS129 α-synuclein; 1:250; Millipore) and NG2 (1:300; Millipore) after autoclaving at 105 °C for 10 min.

Bielschowsky's silver staining was done using deparaffinized sections. Slides were incubated in 40 °C 20% (wt/vol) silver nitrate (Thermo Fisher) for 16 min before 3 washes in distilled H_2O. Ammonium hydroxide (Acros Organics) was added to the silver nitrate solution until the precipitate formed was clear. Slides were incubated in the ammonium silver solution for 30 min at 40 °C before moving to developer working solution for 1 min. Developer working solution was made fresh by adding 8 drops concentrated ammonium hydroxide and 8 drops developer stock solution to 50 mL distilled H_2O. Developer stock solution was made fresh by adding 20 mL of 37–40% formaldehyde (Sigma), 0.5 g sodium citrate tribasic dihydrate (Sigma), and 2 drops 70% nitric acid (Sigma) to 100 mL distilled H_2O. Slides were dipped in 1% (vol/vol) ammonium hydroxide solution for 1 min before washing 3 times in distilled H_2O. The slides were incubated in 5% (wt/vol) sodium thiosulfate solution for 5 min before again washing 3 times in distilled H_2O. Finally, slides were dehydrated through graded alcohols and cleared with xylene before mounting.

Slides were imaged using the Zeiss AxioScan.Z1. Digital images were analyzed using the Zen Analysis software package (Zeiss). To quantify α-synuclein neuropathology, a pixel intensity threshold was determined using a positive control slide, which was then applied to all slides. Regions of interest were drawn around the caudoputamen, hippocampus and fimbria, piriform cortex and amygdala, sensory cortex, thalamus, hypothalamus, parahippocampal cortex, and pons in the Tg(*SNCA*)Nbm mice. Regions of interest were drawn around the hippocampus, thalamus, hypothalamus, midbrain, and pons in the TgM83$^{+/-}$ mice. The regions selected for each model were based on the distribution of neuropathology specific to the Tg mouse line. The percentage of pixels positive for staining in each region was determined.

Guanidine hydrochloride denaturation

Guanidine hydrochloride (GnHCl) denaturation of brain homogenates was performed as previously reported [41]. The resulting protein pellets were resuspended in 40 μL 1×NuPAGE LDS loading buffer and boiled for 10 min prior to immunoblotting.

Immunoblotting

Brain homogenates from 2-month-old TgM83$^{+/-}$, Tg(*SNCA*$^{+/+}$)Nbm, Tg(*SNCA*A30P$^{+/+}$)Nbm, and Tg(*SNCA*A53T$^{+/+}$)Nbm mice were clarified by centrifuging for 5 min at 1000×*g*. The supernatant was collected, total protein was measured using the bicinchoninic acid assay (Pierce), and samples were adjusted to 1 mg/mL total protein. Samples were loaded onto a 10% Bolt Bis–Tris gel, and sodium dodecyl sulfate polyacrylamide gel electrophoresis

(SDS-PAGE) was performed using the MES buffer system. Protein was transferred to a nitrocellulose membrane. The membrane was blocked in Odyssey blocking buffer (LiCor) for 1 h at room temperature. Incubation with anti-vinculin (1:10,000; Abcam) and Clone 42 (1:1000; BD Biosciences) was in Odyssey block buffer with 0.2% Tween 20 overnight at 4 °C. Membranes were washed three times with 1× Tris-buffered saline with Tween 20 (TBST) before incubating with near-infrared secondary antibodies (IRDye Goat anti-Mouse-680RD and IRDye Goat anti-Rabbit-800CW, respectively; 1:20,000; LiCor) diluted in Odyssey block buffer with 0.2% Tween 20 and 0.1% SDS for 1 h at room temperature. After washing the blot three times in 1× TBST, the membrane was washed a final time in 1× TBS prior to imaging using the Odyssey Fc (LiCor). Blots were analyzed using Image Studio software (LiCor), employing the TgM83$^{+/-}$ bands to standardize the data.

GnHCl samples were loaded onto a 10% Novex Bis–Tris gel (Thermo Fisher). SDS-PAGE was performed using the MES buffer system. Protein was transferred to a polyvinylidene fluoride (PVDF) membrane. Membranes were blocked in blocking buffer [5% (wt/vol) nonfat milk in 1× TBST] for 1 h at room temperature. Primary antibody incubation (EP1536Y; 1:4000; Abcam) was in blocking buffer overnight at 4 °C. Membranes were washed three times with 1× TBST before incubating with horseradish peroxidase-conjugated goat anti-rabbit secondary antibody (1:10,000; Bio-Rad) diluted in blocking buffer for 1 h at room temperature. After washing blots three times in 1× TBST, membranes were developed using the enhanced chemiluminescent detection system (GE Healthcare) for exposure to X-ray film. Blots were analyzed via ImageJ, using the 0 *M* GnHCl sample to standardize the data.

Statistical analysis

Data are presented as mean ± standard deviation. Analysis of data collected from the α-syn140*A53T–YFP cell assay measuring spontaneous α-synuclein prion formation was done using a Kruskal–Wallis test with a Dunn's multiple comparison post hoc test. Statistical analysis of data collected from the α-syn140*A53T–YFP cell assay comparing control- and MSA-inoculated Tg(*SNCA*)Nbm mice was done by averaging values from mice inoculated with each sample. The average for each of the five control samples and the five MSA samples used in each Tg mouse line was compared using a Mann–Whitney test. The same analysis was performed comparing Tg(*SNCA*A53T$^{+/+}$)Nbm mice inoculated with control or PD patient samples. Mouse neuropathology was analyzed using a two-tailed Student's *t* test with unequal variance to compare MSA-inoculated mice that contained α-synuclein prions with C2-inoculated mice by brain region. Kaplan–Meier curves in the TgM83$^{+/-}$ mice

were analyzed using a log-rank Mantel–Cox test. Comparison of α-syn140*A53T–YFP cell assay data from the serial passaging studies in the TgM83$^{+/-}$ and Tg($SNCA$*A53T$^{+/+}$) Nbm mice was analyzed using a one-way ANOVA with a Dunnett multiple comparison post hoc test. Significance was determined with a P value < 0.05.

Results

Tg($SNCA$)Nbm mice do not develop spontaneous α-synuclein prions

Tg($SNCA$)Nbm mice are homozygous for either WT or mutant (A30P or A53T) α-synuclein and are maintained on an endogenous α-synuclein knockout background ($Snca^{-/-}$) [17]. These animals were reported to develop robust alterations in the enteric nervous system, including accumulation of α-synuclein aggregates resistant to proteinase K. Interestingly, while we were previously unable to induce neurological disease in Tg($SNCA^{+/+}$)Nbm mice following inoculation with brain homogenate from two MSA patient samples [31], others reported that inoculation of sarkosyl-insoluble preparations from MSA patient samples induced widespread α-synuclein neuropathology in these mice 9 months post-inoculation [1]. Comparing the three Tg($SNCA$)Nbm mouse models with TgM83$^{+/-}$ mice [5], which develop neurological disease ~120 days after MSA inoculation [31, 40, 42], we measured total α-synuclein expression in

the brains of 2-month-old TgM83$^{+/-}$, Tg($SNCA^{+/+}$)Nbm, Tg($SNCA$*A30P$^{+/+}$)Nbm, and Tg($SNCA$*A53T$^{+/+}$)Nbm animals (Online Resource, Figs. S1a, b). Among the four models, hemizygous TgM83 mice express the most human α-synuclein while Tg($SNCA$*A53T$^{+/+}$)Nbm mice express the least. Fixed brain sections from aged Tg($SNCA$)Nbm mice (> 450 days old) assessed for accumulation of phosphorylated α-synuclein neuropathology showed these animals do not develop spontaneous inclusions (Online Resource, Fig. S1c). Frozen tissue from the same mice was homogenized and tested for α-synuclein prion formation using the α-syn140*A53T–YFP cell line [43] (Online Resource, Fig. S1d). In this assay, human embryonic kidney (HEK) cells are used to express full-length human α-synuclein with the A53T mutation fused to yellow fluorescent protein (YFP). Samples containing α-synuclein prions infect the cells and induce YFP-positive inclusions, indicated by the dotted line at 10×10^3 A.U.. None of the three aged Tg($SNCA$)Nbm models developed spontaneous α-synuclein prions (WT: 1.6 ± 0.5; A30P: 1.7 ± 0.4; A53T: $1.6 \pm 0.5 \times 10^3$ A.U.).

Tg($SNCA$*A53T$^{+/+}$)Nbm mice propagate MSA prions

Eight-week-old Tg($SNCA^{+/+}$)Nbm, Tg($SNCA$*A30P$^{+/+}$) Nbm, and Tg($SNCA$*A53T$^{+/+}$)Nbm mice were inoculated with brain homogenate from control (C2, C3, C14, C16, and C17) or MSA (MSA6, MSA13, MSA16, MSA17, and MSA18) patient samples (Table 1; Fig. 1a; and Online

Table 1 Efficiency of MSA transmission to Tg($SNCA$) mice

Patient sample	TgM83$^{+/-}$			Tg($SNCA^{+/+}$)Nbm			Tg($SNCA$*A30P$^{+/+}$) Nbm			Tg($SNCA$*A53T$^{+/+}$) Nbm		
	F	M	n/n_0	F	M	n/n_0	F	M	n/n_0	F	M	n/n_0
C2	8	4	0/12	4	3	0/7	4	4	0/8	4	3	0/7
C3	–	–	n.d.	4	4	0/8	4	4	0/8	4	4	0/8
C14	0	8	0/8	3	4	0/7	4	4	0/8	4	4	0/8
C16	–	–	n.d.	4	4	0/8	4	4	0/8	4	4	0/8
C17	–	–	n.d.	4	4	0/8	4	4	0/8	4	4	0/8
MSA6	4	4	8/8	4	4	0/8	4	4	0/8	4	3	7/7
MSA13	3	5	8/8	3	4	0/7	4	4	0/8	4	4	7/8
MSA16	–	–	n.d.	2	4	0/6	4	3	0/7	3	4	4/7
MSA17	6	3	9/9	4	4	0/8	4	4	0/8	4	4	2/8
MSA18	4	4	8/8	4	4	0/8	4	4	1/8	4	4	3/8
[C2][a]	8	8	0/16	–	–	n.d.	–	–	n.d.	6	5	0/11
[MSA6][a]	8	8	15/16	–	–	n.d.	–	–	n.d.	6	5	5/11
[MSA13][a]	8	7	13/15	–	–	n.d.	–	–	n.d.	7	8	2/15

F number of female mice inoculated, M number of male mice inoculated, n number of affected mice, n_0 number of inoculated mice, $n.d.$ not determined

[a][Samples] indicate human patient samples passaged either in TgM83$^{+/-}$ mice and inoculated in Tg($SNCA$*A53T$^{+/+}$)Nbm animals or passaged in Tg($SNCA$*A53T$^{+/+}$)Nbm mice prior to inoculating in TgM83$^{+/-}$ animals
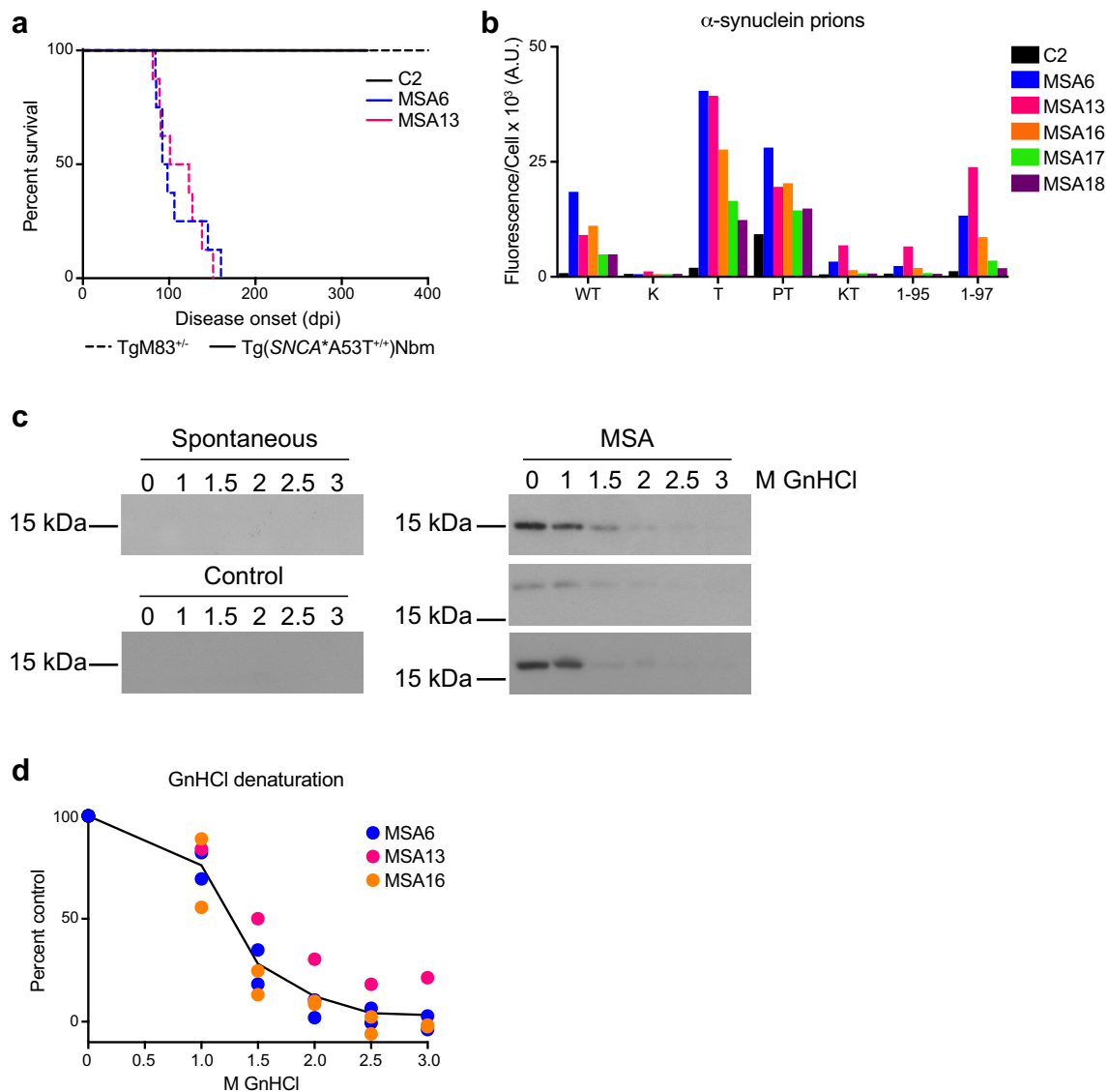
Fig. 1 MSA prions retain biological and biochemical properties after passing in Tg(*SNCA**A53T^+/+)Nbm mice. **a** Kaplan–Meier plot of disease onset in TgM83^+/− (dotted lines) and Tg(*SNCA**A53T^+/+)Nbm mice (solid lines) inoculated with either control sample C2 or MSA patient samples MSA6 and MSA13. TgM83^+/− mice inoculated with MSA6 and MSA13 developed neurological disease (incubation times in Online Resource, Table S2; data previously reported in [31]). Tg(*SNCA**A53T^+/+)Nbm did not develop overt motor signs by 330 dpi. **b–d** Brain homogenate from Tg(*SNCA**A53T^+/+)Nbm mice that propagated MSA prions, as well as mice inoculated with control sample C2, were assessed for **b** biological and **c, d** biochemical properties of MSA prions. **b** Alpha-synuclein prions were isolated from brain homogenates via PTA precipitation and were incubated with α-syn–YFP cells for 4 days. Homogenates from MSA-inoculated mice showed poor infectivity in cells expressing the E46K mutation alone or in combination with the A53T mutation and were unable to propagate well in cells truncated at residue 95. Homogenates from mice inoculated with sample C2 showed no infectivity. Cell lines express WT α-syn140–YFP, single mutations [A30P (P), E46K (K), and A53T (T)], double mutations [A30P,A53T (PT) and E46K,A53T (KT)], or A53T truncated at residue 95 (1–95) or 97 (1–97). **c, d** Alpha-synuclein prions in MSA-inoculated mice were denatured using increasing concentrations of GnHCl. Representative blots using the EP1536Y primary antibody are shown in **c**. No insoluble protein was detected in aged Tg(*SNCA**A53T^+/+)Nbm mice or animals inoculated with C2 homogenate

Resource, Table S2). Unlike TgM83^+/− mice, which develop neurological disease ~120 days after MSA inoculation, the Tg(*SNCA*)Nbm animals remained asymptomatic for > 330 dpi. Tg(*SNCA*^+/+)Nbm mice were euthanized 400 dpi while Tg(*SNCA**A30P^+/+)Nbm and Tg(*SNCA**A53T^+/+)Nbm mice were euthanized 330 dpi. The left hemisphere of the brain was collected frozen from each animal, and a 10% brain homogenate was prepared. Alpha-synuclein aggregates were isolated by PTA precipitation [34], and the resulting protein pellets were tested for infectivity

using the α-syn140*A53T–YFP cell assay (Table 2). Alpha-synuclein isolated from the Tg(SNCA⁺/⁺)Nbm mice inoculated with either control or MSA patient samples did not infect the cells (P > 1). Additionally, only one Tg(SNCA*A30P⁺/⁺)Nbm mouse inoculated with patient sample MSA18 infected the α-syn140*A53T–YFP cells (P = 0.31). However, brain homogenate from the majority of Tg(SNCA*A53T⁺/⁺)Nbm mice inoculated with MSA infected the α-syn140*A53T–YFP cells, demonstrating that MSA prions can propagate in A53T-expressing mice (P < 0.01).

MSA prions propagate in Tg(*SNCA**A53T⁺/⁺)Nbm mice with high fidelity

Previously, we built a panel of HEK cells expressing α-synuclein containing various mutations and truncations [41]. Using these cells, we showed that MSA prions are unable to replicate in the presence of the PD-causing E46K mutation. Additionally, truncating α-syn*A53T at amino acid residue 95 also blocked in vitro propagation of MSA prions. To confirm the misfolded conformation, or strain, of α-synuclein in MSA patients propagates with high fidelity in Tg(SNCA*A53T⁺/⁺)Nbm mice, we tested brain homogenates from mice positive for α-synuclein infection in each of the seven cell lines represented in our panel: WT (α-syn140–YFP), E46K (α-syn140*E46K–YFP), A53T (α-syn140*A53T–YFP), A30P and A53T (α-syn140*A30P,A53T–YFP), E46K and A53T (α-syn140*E46K,A53T–YFP), A53T truncated at residue 95 (α-syn95*A53T–YFP), and A53T truncated at residue 97 (α-syn97*A53T–YFP). Homogenates from mice inoculated with control sample C2 did not infect any of the α-syn–YFP cell lines (Fig. 1b). In contrast, homogenates from MSA-inoculated mice that were positive for α-synuclein

prions did infect α-syn140*–YFP, α-syn140*A53T–YFP, α-syn140*A30P,A53T–YFP, and α-syn97*A53T–YFP cells, but did not infect the α-syn140*E46K–YFP, α-syn140*E46K,A53T–YFP, or the α-syn95*A53T–YFP cell lines. These data demonstrate that MSA prions retain their biological activity after passaging in Tg(SNCA*A53T⁺/⁺)Nbm mice.

We biochemically characterized α-synuclein prions isolated from Tg(SNCA*A53T⁺/⁺)Nbm mice using GnHCl denaturation. Previously, we reported that MSA prions are ~50% denatured by 1.5 M GnHCl and completely denatured by 3 M GnHCl [41]. Here, we also found that α-synuclein aggregates from MSA-inoculated Tg(SNCA*A53T⁺/⁺) Nbm mice are fully denatured by 3 M GnHCl and ~50% denatured in 1.5 M GnHCl (Fig. 1c, d). Notably, neither aged Tg(SNCA*A53T⁺/⁺)Nbm nor control-inoculated Tg(SNCA*A53T⁺/⁺)Nbm mice developed insoluble α-synuclein inclusions (Fig. 1c).
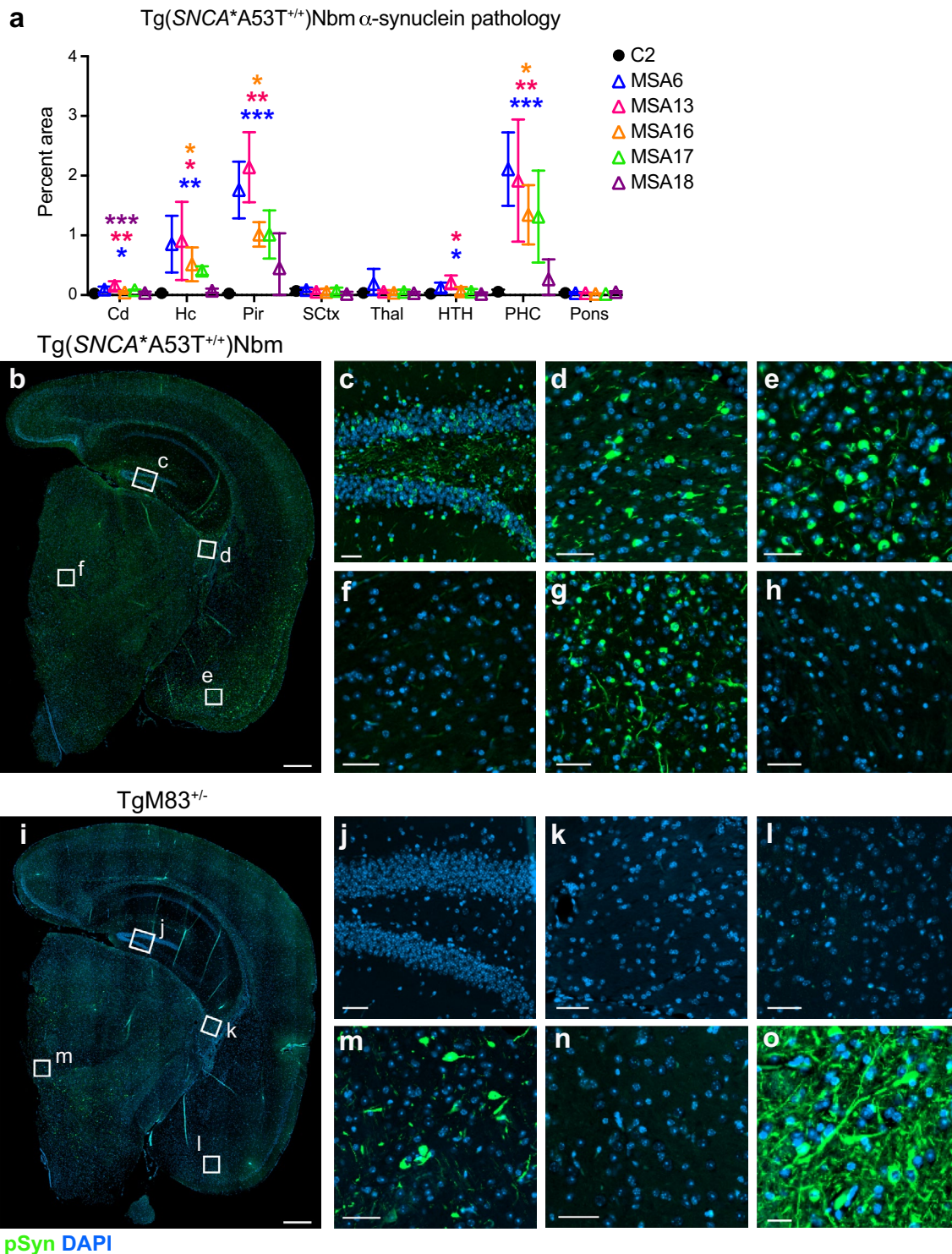
MSA-inoculated Tg(*SNCA**A53T⁺/⁺)Nbm mice develop α-synuclein neuropathology in the limbic system

Fixed half-brains from inoculated Tg(SNCA)Nbm mice were analyzed for the presence of phosphorylated α-synuclein aggregates via immunofluorescence. Eight micron sections were cut and stained with the EP1536Y primary antibody for α-synuclein phosphorylated at residue Ser129. Consistent with the previous results, neither Tg(SNCA ⁺/⁺)Nbm nor Tg(SNCA*A30P⁺/⁺)Nbm mice inoculated with MSA developed α-synuclein neuropathology (Online Resource, Figs. S2a, b). However, fixed tissue from Tg(SNCA*A53T⁺/⁺) Nbm mice that were positive for MSA prions in the cell assay did develop α-synuclein aggregates in the hippocampus and fimbria (Hc), the piriform cortex and amygdala (Pir), and the parahippocampal cortex (PHC; Fig. 2a–h).

Table 2 MSA prion propagation in Tg(*SNCA*) mice

Patient sample	Mean cell infection ± SD, fluorescence/cell (×10³ A.U.)[a]		
	Tg(*SNCA*⁺/⁺)Nbm	Tg(*SNCA**A30P⁺/⁺)Nbm	Tg(*SNCA**A53T⁺/⁺)Nbm
C2	2.4 ± 1.0	1.6 ± 0.3	1.8 ± 0.8
C3	2.4 ± 1.0	2.0 ± 0.9	2.1 ± 1.0
C14	1.4 ± 0.3	1.9 ± 0.5	3.3 ± 3.5
C16	2.4 ± 1.0	1.9 ± 0.5	2.0 ± 0.6
C17	1.3 ± 0.4	1.7 ± 0.5	2.1 ± 0.4
MSA6	1.9 ± 0.4	3.3 ± 1.8	78 ± 12
MSA13	2.3 ± 0.6	1.8 ± 0.4	39 ± 22
MSA16	1.8 ± 0.3	2.3 ± 1.1	29 ± 26
MSA17	1.6 ± 0.7	1.7 ± 0.5	13 ± 16
MSA18	1.3 ± 0.1	4.0 ± 6.2	9.2 ± 10

[a]Measurements made from five images per well, n = 6 wells. PTA-precipitated samples were diluted in DPBS 1:10 before testing on α-syn140*A53T–YFP cells

This predominantly limbic pathology was absent in mice inoculated with control sample C2. Notably, the distribution of α-synuclein inclusions in Tg(*SNCA**A53T^+/+)Nbm mice is in stark contrast to the hindbrain neuropathology that develops in MSA-inoculated TgM83^+/− mice (Fig. 2i–o). Whereas TgM83^+/− mice developed inclusions in the thalamus (Fig. 2m) and brainstem (Fig. 2o), these regions were unaffected in Tg(*SNCA**A53T^+/+)Nbm mice (Fig. 2f, h, respectively). Moreover, the Hc (Fig. 2j), fimbria (Fig. 2k), Pir (Fig. 2l), and PHC (Fig. 2n) were also unaffected in the TgM83^+/− mice. These findings suggest that the difference in neurological presentation between the two models (Fig. 1a)

◀**Fig. 2** Tg(*SNCA**A53T$^{+/+}$)Nbm mice inoculated with MSA develop α-synuclein neuropathology. **a**–**h** Tg(*SNCA**A53T$^{+/+}$)Nbm mice received an intracranial inoculation of 1% brain homogenate from one control or five MSA patient samples. Mice were collected 330 dpi, and fixed half-brains were cut coronally into four sections to allow analysis of phosphorylated α-synuclein inclusions in the caudoputamen (Cd), hippocampus and fimbria (Hc), piriform cortex and amygdala (Pir), sensory cortex (SCtx), thalamus (Thal), hypothalamus (HTH), parahippocampal cortex (PHC), and pons. **a** Tg(*SNCA**A53T$^{+/+}$)Nbm mice positive for MSA prions developed phosphorylated α-synuclein aggregates in the limbic system, whereas control-inoculated mice did not. Pathology was measured from one slide per animal; C2: $n=7$; MSA6: $n=6$; MSA13: $n=5$; MSA16: $n=4$; MSA17: $n=2$; MSA18: $n=3$. **b**–**h** Representative images of α-synuclein pathology in Tg(*SNCA**A53T$^{+/+}$)Nbm mice. **b** Full section including Hc, Pir, SCtx, Thal, and HTH shown with white boxes indicating magnified regions in **c**–**f**. For comparison, **i**–**o** representative images of pathology in a terminal TgM83$^{+/-}$ mouse inoculated with MSA. **i** Full section reveals a distinct staining pattern from **b**. Higher magnification images show Hc (**c**, **j**), fimbria (**d**, **k**), Pir (**e**, **l**), Thal (**f**, **m**), PHC (**g**, **n**), and brainstem (**h**, **o**). Phosphorylated α-synuclein in green; DAPI in blue. Scale bars in **b**, **i**, 500 μm; all others, 50 μm. *$P<0.05$; **$P<0.01$; ***$P<0.001$

Fig. 3 Tg(*SNCA**A53T$^{+/+}$)Nbm mice develop silver-positive aggregates. One slide from four MSA-inoculated Tg(*SNCA**A53T$^{+/+}$)Nbm mice with phosphorylated α-synuclein neuropathology were analyzed for the presence of silver-positive aggregates. Representative full section (**a**) shows magnified regions of the hippocampus (**b**) and piriform cortex (**c**) in black boxes, which contain labeled aggregates. Scale bar in **a**, 500 μm. Scale bars in **b**, **c**, 50 μm

is likely due to differences in the brain regions affected by MSA inoculation.

Tg(*SNCA**A53T$^{+/+}$)Nbm mice were also inoculated with brain homogenate from five PD patient samples. Mice collected 330 dpi showed no phosphorylated α-synuclein pathology (data from mice inoculated with sample PD6 shown in Online Resource, Fig. S2c). Similarly, no α-synuclein prions were detected in PD-inoculated mice using the α-syn140*A53T–YFP cell assay (Online Resource, Table S3).

Tg(*SNCA**A53T$^{+/+}$)Nbm mice inoculated with MSA develop neuronal and glial pathology

Bielschowsky's silver staining on Tg(*SNCA**A53T$^{+/+}$) Nbm mice inoculated with MSA patient samples revealed silver-positive aggregates in the Hc and Pir (Fig. 3). Given this distinct distribution of inclusions, compared to the TgM83$^{+/-}$ mice, we were interested in determining which cell type(s) developed α-synuclein aggregates. We performed co-localization studies with the neuronal marker MAP2 in both Tg(*SNCA**A53T$^{+/+}$)Nbm and TgM83$^{+/-}$ mice inoculated with MSA (Fig. 4). As expected, TgM83$^{+/-}$ mice, which use the mouse prion protein promoter to drive transgene expression, developed inclusions that co-localized with MAP2 staining (Fig. 4d, e; arrows in bottom panel of Fig. 4e identify co-labeling). We also observed MAP2 co-localization with α-synuclein in the Hc and Pir of Tg(*SNCA**A53T$^{+/+}$)Nbm mice (Fig. 4a–c; arrows in bottom panels of Fig. 4b, c show co-labeling). However, a number of α-synuclein aggregates did not co-localize with MAP2 (arrowheads in the bottom panels of Fig. 4b, c),
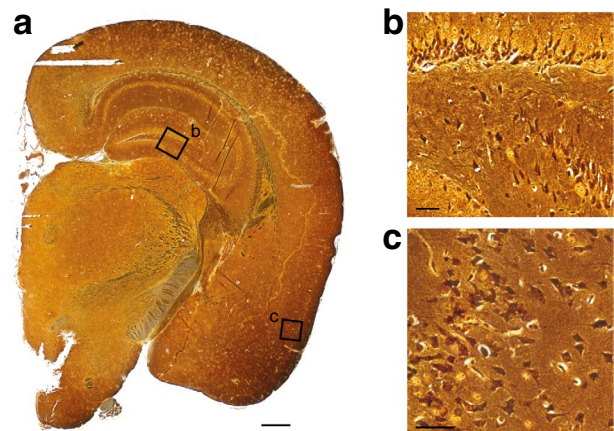
indicating α-synuclein inclusions form in multiple cell types in Tg(*SNCA**A53T$^{+/+}$)Nbm mice.

To determine which additional cells contained α-synuclein aggregates, we performed co-localization studies using antibodies specific for three glial cell types (Figs. 5, 6). The neuronal α-synuclein aggregates in TgM83$^{+/-}$ mice were proximal to reactive astrocytes (GFAP; Fig. 5c) and microglia (Iba1; Fig. 5f), but as expected, none of the α-synuclein co-localized with either cell type in these mice (bottom panels). Alternatively, while some of the phosphorylated α-synuclein aggregates in the Tg(*SNCA**A53T$^{+/+}$) Nbm animals co-localized with microglia (indicated by arrows in Fig. 5d, e), the vast majority were found in astrocytes (indicated by arrows in Fig. 5a, b). Given that MSA is defined by the presence of GCIs in oligodendrocytes, we also assessed the co-localization of α-synuclein with oligodendrocytes using the cell-specific marker Olig2 (Fig. 6). Alpha-synuclein inclusions in TgM83$^{+/-}$ mice did not co-localize with Olig2 immunostaining (Fig. 6c), but a small number of inclusions in the Hc and Pir of Tg(*SNCA**A53T$^{+/+}$)Nbm mice did (arrows in Fig. 5a, b).

In addition to immunostaining results from the two Tg mouse models, we also analyzed fixed tissue from two MSA patient samples (MSA46 and MSA47; Online Resource, Fig. S3). In line with reports of neuronal α-synuclein inclusions in MSA patients [12, 25, 29], we observed some co-localization of α-synuclein with MAP2 (Online Resource, Fig. S3a). Looking at glial cells, we also identified a number of α-synuclein inclusions in astrocytes and microglia (Online Resource, Fig. S3b); however, as expected, α-synuclein

Fig. 4 Tg(*SNCA**A53T)Nbm mice inoculated with MSA develop neuronal pathology. Formalin-fixed half-brains from **a–c** Tg(*SNCA**A53T$^{+/+}$)Nbm ($n = 21$) and **d–e** TgM83$^{+/-}$ mice ($n = 2$) inoculated with MSA brain homogenate were analyzed for co-localization of α-synuclein (green) with the neuronal marker MAP2 (purple). One slide per animal was assessed. **a, d** White boxes in low-magnification images identify regions of the hippocampus (i) and piriform cortex (ii) from Tg(*SNCA**A53T$^{+/+}$)Nbm mice and the brainstem (iii) from TgM83$^{+/-}$ mice. All regions are shown in higher magnification in the panels below as well as in Figs. 5 and 6. **b, c, e** Alpha-synuclein pathology (top panels) and MAP2 immunostaining (middle panels) co-localized in both mouse models (white, bottom panels). Arrows point to α-synuclein aggregates that co-localize with MAP2. Arrowheads identify non-neuronal α-synuclein aggregates. Images shown from the **b** hippocampus, **c** piriform cortex, and **e** brainstem. DAPI in blue. Scale bars in **a, d**, 500 μm. Scale bars in **b, c, e**, 50 μm
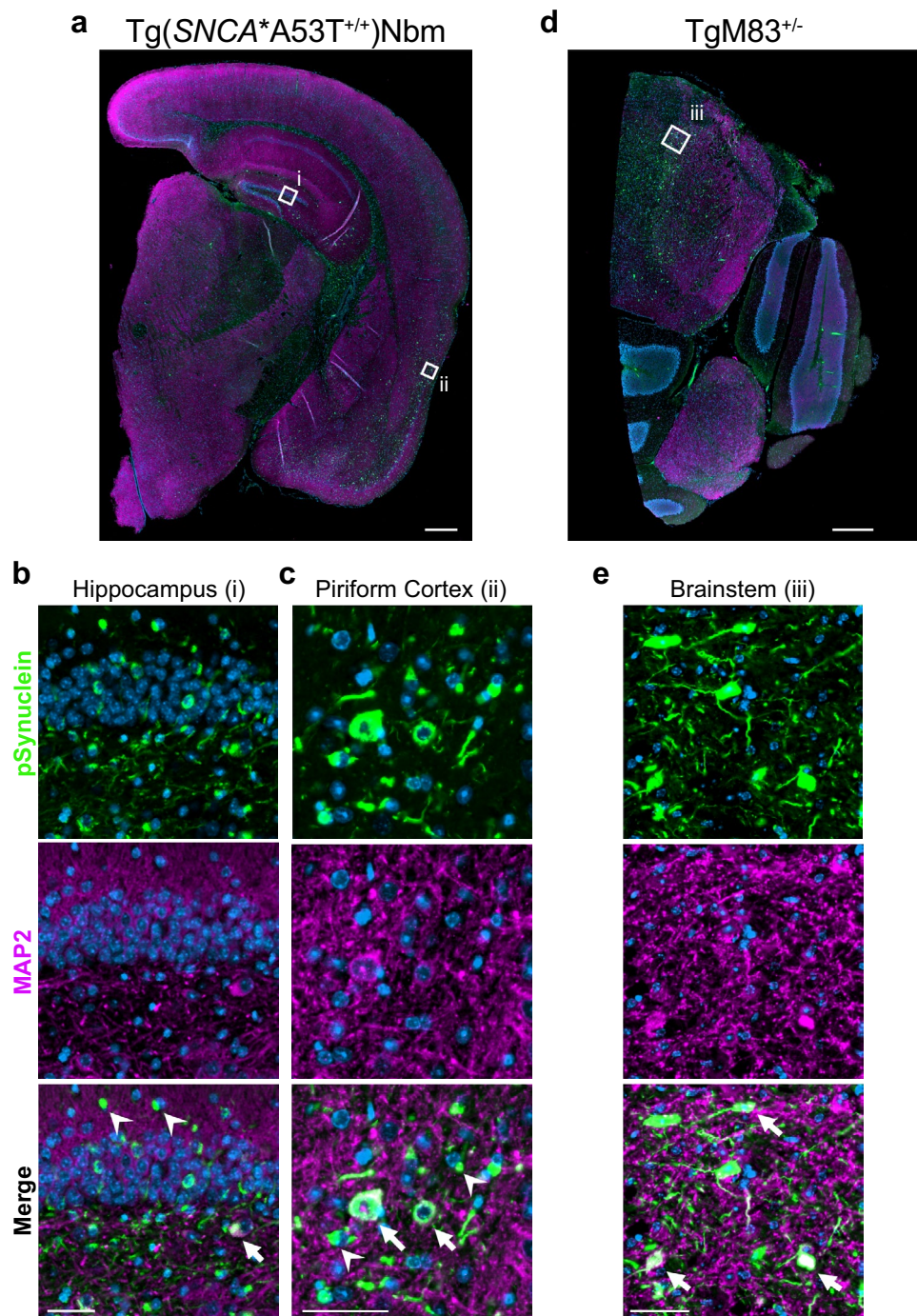
predominantly aggregated in oligodendrocytes (Online Resource, Fig. S3c).

Intrigued by the finding that α-synuclein pathology in Tg(*SNCA**A53T$^{+/+}$)Nbm mice is frequently found in astrocytes, as well as a handful of oligodendrocytes, we analyzed both Tg mouse models and human samples for co-localization with NG2 immunostaining (Online Resource, Fig. S4). NG2 cells are polydendrocytes and are the fourth major glial cell type in the brain constituting 2–8% of cells in the adult CNS [26]. While NG2 cells were initially thought to only give rise to oligodendrocytes [3, 16, 32, 45, 48], it is now known they can also differentiate into astrocytes [10, 47, 48]. Recently, two groups reported co-localization of α-synuclein neuropathology with NG2 cells in MSA patient samples [15, 24]. Using immunofluorescence with an NG2-specific antibody to determine co-localization with α-synuclein, we found that neither Tg mouse model developed α-synuclein inclusions in NG2 cells (Online Resource,

Fig. 5 Tg(*SNCA**A53T$^{+/+}$) Nbm mice inoculated with MSA develop glial pathology. Fixed tissue from both Tg(*SNCA**A53T$^{+/+}$)Nbm ($n=21$) and TgM83$^{+/-}$ mice ($n=2$) inoculated with MSA patient samples was analyzed for α-synuclein co-localization with **a–c** astrocytes and **d–f** microglia. One slide per animal was assessed. (**a–c**) Immunostaining for phosphorylated α-synuclein (green, top panels) and astrocytes (GFAP; purple, middle panels) shown from the **a** hippocampus and **b** piriform cortex of Tg(*SNCA**A53T$^{+/+}$) Nbm mice and the **c** brainstem of TgM83$^{+/-}$ mice, as identified in Fig. 4a, d. Merged images (bottom panels) show co-localization of α-synuclein with GFAP in Tg(*SNCA**A53T$^{+/+}$) Nbm mice (arrows identify co-labeling in white), whereas no co-staining was seen in TgM83$^{+/-}$ mice. **d–f** The same sections were also analyzed for α-synuclein (top panels) co-localization with microglia (Iba1; red, middle panels). Some co-labeling (white, bottom panels) was seen in Tg(*SNCA**A53T$^{+/+}$)Nbm mice (white arrows), but no co-localization was observed in TgM83$^{+/-}$ mice. DAPI in blue. Scale bars, 50 μm
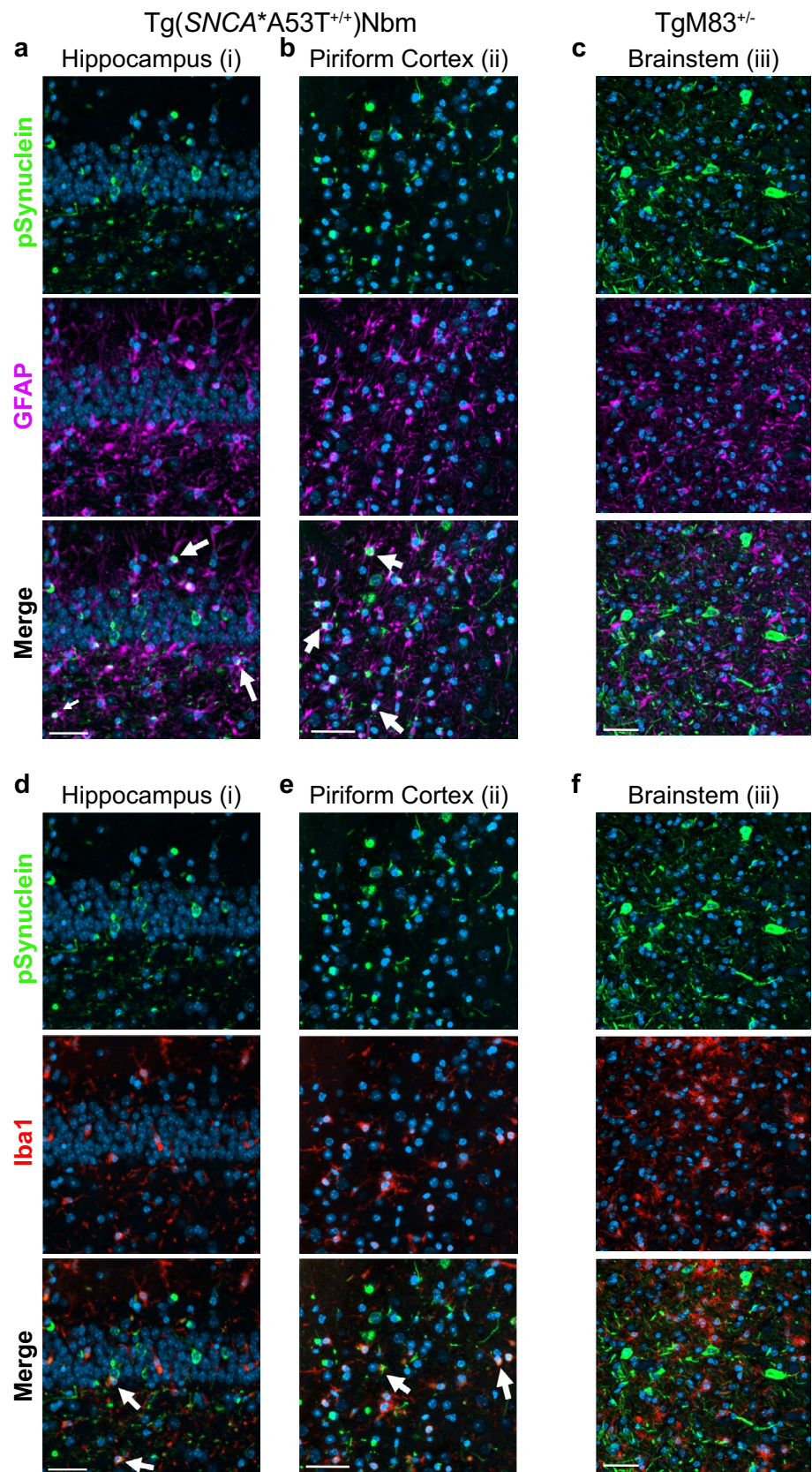
Fig. 6 Tg(*SNCA**A53T$^{+/+}$) Nbm mice inoculated with MSA develop oligodendroglial inclusions. Fixed tissue from both Tg(*SNCA**A53T$^{+/+}$)Nbm (*n* = 10) and TgM83$^{+/-}$ mice (*n* = 2) inoculated with MSA patient samples were analyzed for α-synuclein (green, top panels) co-localization with oligodendrocytes (Olig2; red, middle panels). Some oligo-dendroglial inclusions (bottom panels show merged images) were seen in the **a** hippocampus and **b** piriform cortex of Tg(*SNCA**A53T$^{+/+}$)Nbm mice, but none were seen in the **c** brainstem of TgM83$^{+/-}$ mice. One slide per animal was assessed. Scale bars, 50 μm
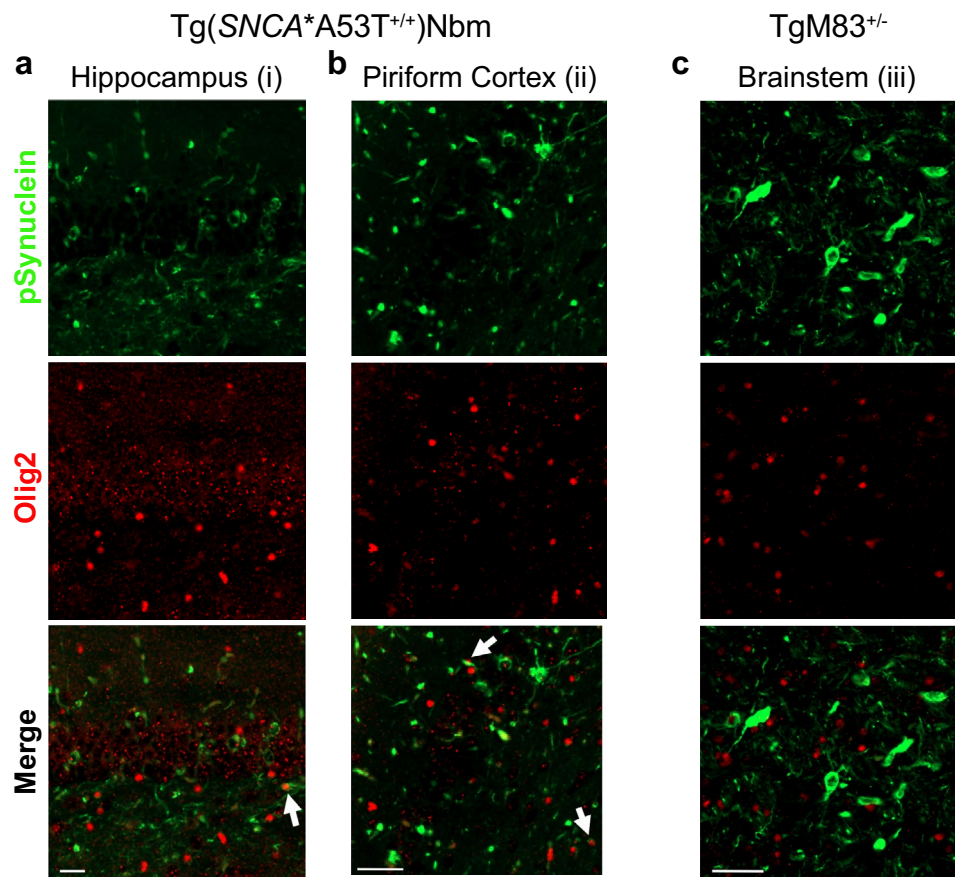
Fig. S4a). However, both MSA patient samples showed co-localization of phosphorylated α-synuclein with NG2 immunolabeling, though more co-staining was observed in patient MSA46 than MSA47, which may be due to differences in the clinical presentation between the two patients (MSA46 was diagnosed with the cerebellar phenotype while MSA47 was diagnosed with the parkinsonian phenotype; Online Resource, Fig. S4b). Confirming that the two MSA patient samples used for the immunofluorescence studies were consistent with the frozen tissue used to inoculate the Tg(*SNCA**A53T$^{+/+}$)Nbm mice, we isolated α-synuclein prions from fresh frozen tissue via PTA-precipitation from the same brain region from both patient samples. We then tested the α-synuclein prions for biological activity by incubating the samples with our panel of α-syn–YFP cell lines (Online Resource, Fig. S5). Consistent with our previous findings [41] and additional data reported here, the samples were able to selectively infect the α-syn–YFP cells, with the exception of lines expressing the E46K mutation or truncation of the protein at residue 95.

MSA prions propagated in Tg(*SNCA**A53T$^{+/+}$)Nbm mice transmit disease to TgM83$^{+/-}$ animals

Observing that MSA prions retain their biological and biochemical properties upon inoculation, or passaging, in Tg(*SNCA**A53T$^{+/+}$)Nbm mice, we proposed the brain homogenates from these animals would transmit disease to TgM83$^{+/-}$ mice. To address this hypothesis, we inoculated 10-week-old TgM83$^{+/-}$ mice with 1% brain homogenate from Tg(*SNCA**A53T$^{+/+}$)Nbm mice originally inoculated with control patient sample C2 or an MSA patient sample (MSA6 or MSA13). TgM83$^{+/-}$ mice inoculated with passaged C2 brain homogenate remained asymptomatic 450 dpi (Fig. 7a); however, mice inoculated with brain homogenate from either MSA6 or MSA13 patient samples passaged in Tg(*SNCA**A53T$^{+/+}$)Nbm mice developed neurological disease (MSA6: 119 ± 24 dpi; MSA13: 245 ± 85 dpi; $P < 0.0001$). Flash-frozen half-brains from terminal animals were homogenized, and the α-synuclein prion concentration was measured using the α-syn140*A53T–YFP cell assay (Fig. 7b). TgM83$^{+/-}$ mice inoculated with passaged C2 patient sample did not contain α-synuclein prions ($2.9 \pm 1.2 \times 10^3$ A.U.), but animals inoculated with the passaged MSA patient samples were positive for α-synuclein prions (MSA6: 71 ± 30 A.U.; MSA13: $54 \pm 38 \times 10^3$ A.U.;
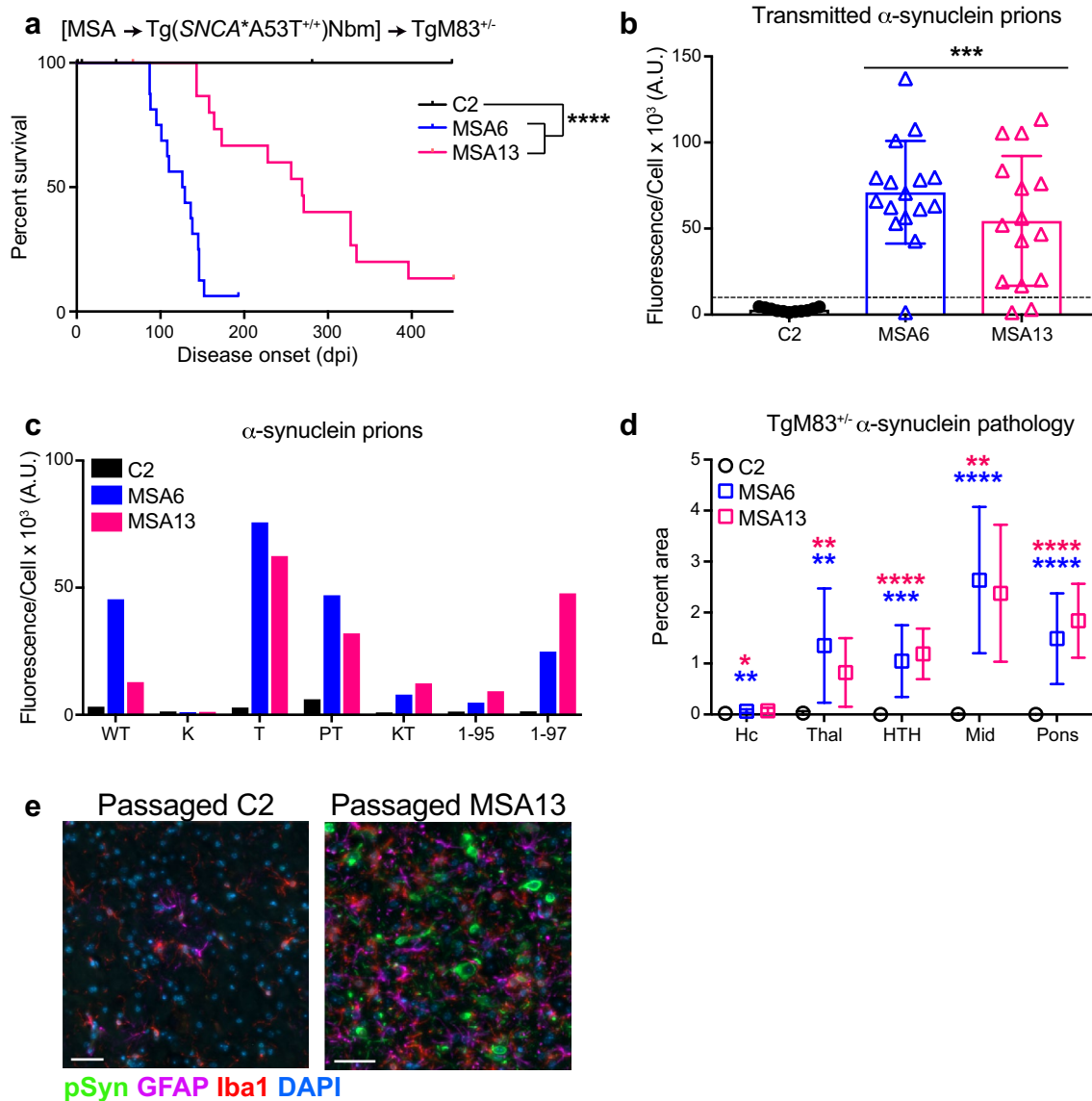
Fig. 7 MSA prions transmit disease to TgM83^{+/−} mice after passaging in Tg(SNCA*A53T^{+/+})Nbm mice. Brain homogenate from Tg(SNCA*A53T^{+/+})Nbm mice inoculated with either control (C2) or MSA (MSA6 or MSA13) patient samples was inoculated into TgM83^{+/−} mice. **a** Mice inoculated with mouse-passaged MSA samples developed neurological disease, whereas mice inoculated with passaged C2 homogenate remained asymptomatic through 450 dpi. **b** Frozen half-brains from inoculated TgM83^{+/−} mice were tested for MSA prions in the α-syn140*A53T–YFP cell assay (×10^{3} A.U.). Inoculation with passaged C2 homogenate did not induce α-synuclein prions (all samples below the dotted line), whereas mouse-passaged MSA samples induced α-synuclein prion formation. **c** Alpha-synuclein prions in TgM83^{+/−} mice were analyzed for infectivity in additional α-syn–YFP cell lines. Samples infected cells expressing WT and mutant α-synuclein (A53T—T; A30P,A53T—PT; and A53T truncated at residue 97—1–97), but they did not infect cells express-ing the E46K mutation alone (K) or in combination with the A53T mutation (KT). Additionally, they did not infect A53T-expressing cells truncated at residue 95 (1–95). **d, e** Fixed half-brains from the same mice were analyzed for phosphorylated α-synuclein neuropathology. Mice inoculated with the mouse-passaged C2 patient sample ($n = 11$) did not develop α-synuclein aggregates, whereas inoculation of passaged MSA patient samples (MSA6: $n = 13$; MSA13: $n = 9$) induced widespread α-synuclein accumulation (green) and reactive astrocytes (GFAP; purple) and microglia (Iba1; red) in the hindbrain. Quantification of α-synuclein in the hippocampus (Hc), thalamus (Thal), hypothalamus (HTH), midbrain (Mid), and pons is shown in **d**. Analysis was performed on one slide containing all brain regions from each animal. Representative images from the brainstem shown in **e**. DAPI in blue. Scale bar, 50 μm. *$P < 0.05$; **$P < 0.01$; ***$P < 0.001$; ****$P < 0.0001$
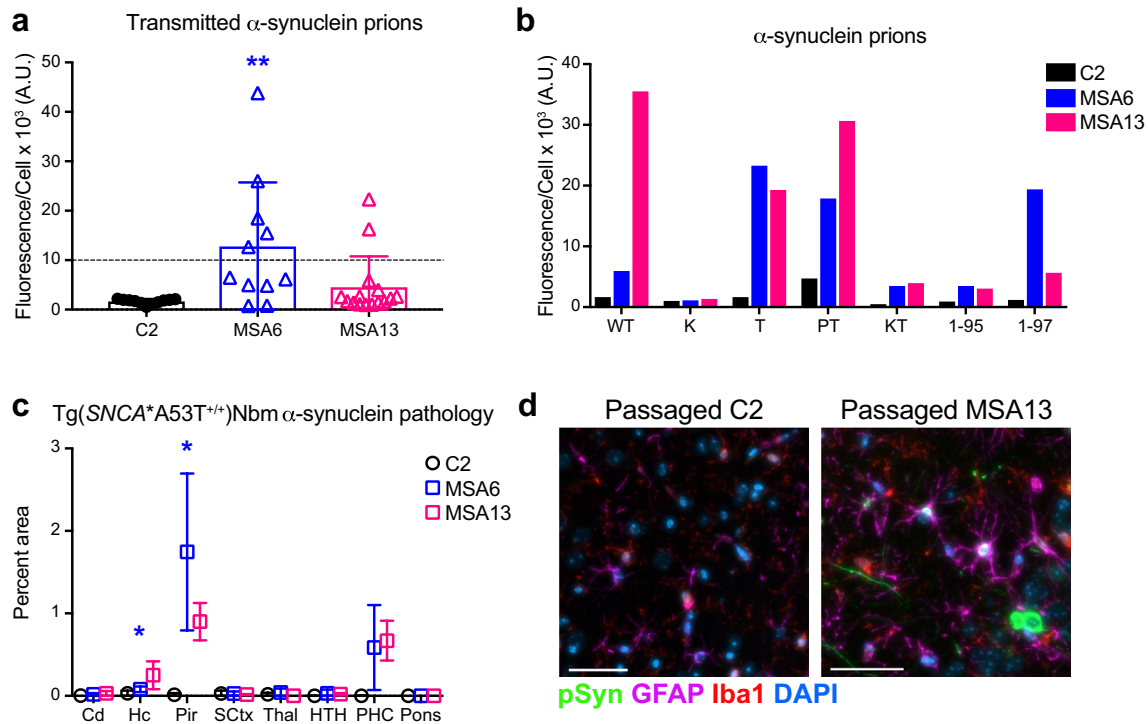
Fig. 8 MSA prions passaged in TgM83^{+/−} mice propagate in Tg(*SNCA**A53T^{+/+})Nbm animals. Brain homogenates from control (C2) or MSA patient samples (MSA6 or MSA13) first passaged in TgM83^{+/−} mice were used to inoculate Tg(*SNCA**A53T^{+/+})Nbm animals. Mice were collected 300 dpi. **a** Frozen half-brains were homogenized and assessed for the presence of α-synuclein prions using the α-syn140*A53T–YFP cell assay ($\times 10^3$ A.U.). Passaged C2 homogenate did not induce α-synuclein prion formation, but seven mice inoculated with either passaged MSA6 or MSA13 patient samples propagated α-synuclein prions. **b** Alpha-synuclein prions in the Tg(*SNCA**A53T^{+/+})Nbm mice were analyzed for infectivity in additional α-syn–YFP cell lines. Samples infected cells expressing wild-type (WT) and mutant α-synuclein (A53T—T; A30P,A53T—PT; and A53T truncated at residue 97—1–97), but they did not infect cells expressing the E46K mutation alone (K) or in combination with the A53T mutation (KT). Additionally, they did not infect A53T-

expressing cells truncated at residue 95 (1–95). Homogenates from mice inoculated with passaged C2 patient sample did not infect any of the cells. **c, d** Fixed half-brains from the same mice were analyzed for phosphorylated α-synuclein neuropathology in the caudoputamen (Cd), hippocampus and fimbria (Hc), piriform cortex and amygdala (Pir), sensory cortex (SCtx), thalamus (Thal), hypothalamus (HTH), parahippocampal cortex (PHC), and pons. Mice inoculated with passaged C2 patient sample ($n=11$) did not develop α-synuclein aggregates, whereas inoculation of mouse-passaged MSA samples (MSA6: $n=5$; MSA13: $n=2$) induced α-synuclein accumulation in the Pir and PHC. Quantification performed using one slide containing all analyzed brain regions per animal (**c**). Representative images (**d**) show that the passaged MSA patient samples induced α-synuclein inclusions (green) that co-localized with astrocytes (GFAP; purple) and reactive microglia (Iba1; red). DAPI in blue. Scale bar, 50 µm. *$P < 0.01$; **$P < 0.01$

$P < 0.001$). These α-synuclein prions retained biological characteristics of MSA prions. Testing for infectivity in the α-syn–YFP cell panel revealed α-synuclein isolated from TgM83^{+/−} mice inoculated with passaged MSA patient samples infected α-syn140–YFP, α-syn140*A53T–YFP, α-syn140*A30P,A53T–YFP, and α-syn97*A53T–YFP cells, but did not infect cells expressing the E46K mutation or α-synuclein truncated at residue 95 (Fig. 7c). These data argue MSA prions propagate with high fidelity between two Tg(*SNCA**A53T) mouse models.

We also assessed the formalin-fixed half-brains from the same animals. Consistent with our cell assay data, we found that serial passaging of the two MSA patient samples induced α-synuclein inclusions in the hindbrain of

TgM83^{+/−} mice (Fig. 7d, e). However, serial passaging with the control sample C2 did not.

MSA prions from symptomatic TgM83^{+/−} mice propagate in Tg(*SNCA**A53T^{+/+})Nbm animals

In previous studies, TgM83^{+/−} mice inoculated with brain homogenate from MSA patient samples MSA6 and MSA13 induced neurological disease in the animals [42]. Brain homogenates from these mice, as well as from C2-inoculated animals terminated 450 dpi, were used to inoculate Tg(*SNCA**A53T^{+/+})Nbm mice. These animals were collected 300 dpi, and flash-frozen half-brains were tested for the presence of MSA prions using the α-syn140*A53T–YFP cell assay (Fig. 8a). Mice inoculated with the passaged

C2 patient sample did not develop α-synuclein prions ($1.7 \pm 0.5 \times 10^3$ A.U.). However, five mice inoculated with the mouse-passaged MSA6 patient sample ($13 \pm 13 \times 10^3$ A.U., $P < 0.01$) and two mice inoculated with the mouse-passaged MSA13 patient sample ($4.5 \pm 6.2 \times 10^3$ A.U., $P = 0.57$) did contain α-synuclein prions (samples above dotted line). The seven positive samples from serially passaging MSA and the homogenates from the control mice were further tested in the panel of α-syn–YFP cell lines (Fig. 8b). Consistent with the previous passaging data, homogenates from mice inoculated with mouse-passaged MSA patient samples infected the α-syn140–YFP, α-syn140*A53T–YFP, α-syn140*A30P,A53T–YFP, and α-syn97*A53T–YFP cells, but were unable to infect cells expressing the E46K mutation or α-synuclein truncated at residue 95. None of the samples from the mice inoculated with mouse-passaged C2 patient tissue infected the α-syn–YFP cells. These findings demonstrate the biological activity of MSA prions was retained during passaging in both TgM83$^{+/-}$ and Tg(*SNCA**A53T$^{+/+}$) Nbm animals.

Finally, we analyzed the formalin-fixed half-brains from the seven mice positive for MSA prions and the control animals for α-synuclein aggregation via immunostaining (Fig. 8c, d). The control animals did not develop phosphorylated α-synuclein neuropathology, but the mice inoculated with the passaged MSA patient samples developed inclusions in the Pir and PHC. Notably, the hindbrain regions affected in TgM83$^{+/-}$ mice (Fig. 7d) were absent of pathology in the Tg(*SNCA**A53T$^{+/+}$)Nbm animals (Fig. 8c).

Discussion

Over the past 5 years, several studies have demonstrated that TgM83$^{+/-}$ mice inoculated with brain homogenate from MSA patients develop neurological disease ~120 dpi [31, 40–43]. Alternatively, one study using Tg(*SNCA*$^{+/+}$) Nbm mice found the animals remained asymptomatic for > 12 months post-inoculation with MSA homogenates [31], whereas a second study in these animals found insoluble fractions from MSA patient samples induced α-synuclein inclusions within 9 months [1]. To investigate this difference, we inoculated Tg(*SNCA*$^{+/+}$)Nbm mice, as well as animals expressing mutant α-synuclein [Tg(*SNCA**A30P$^{+/+}$)Nbm and Tg(*SNCA**A53T$^{+/+}$) Nbm], with brain homogenate from five MSA patient samples and five control samples. In the absence of neurological signs, mice were terminated either 400 [Tg(*SNCA*$^{+/+}$)Nbm] or 330 dpi [Tg(*SNCA**A30P$^{+/+}$)Nbm and Tg(*SNCA**A53T$^{+/+}$)Nbm]. Using a cell-based assay to detect α-synuclein prions in brain homogenates from the mice [43], we found MSA prions had propagated in
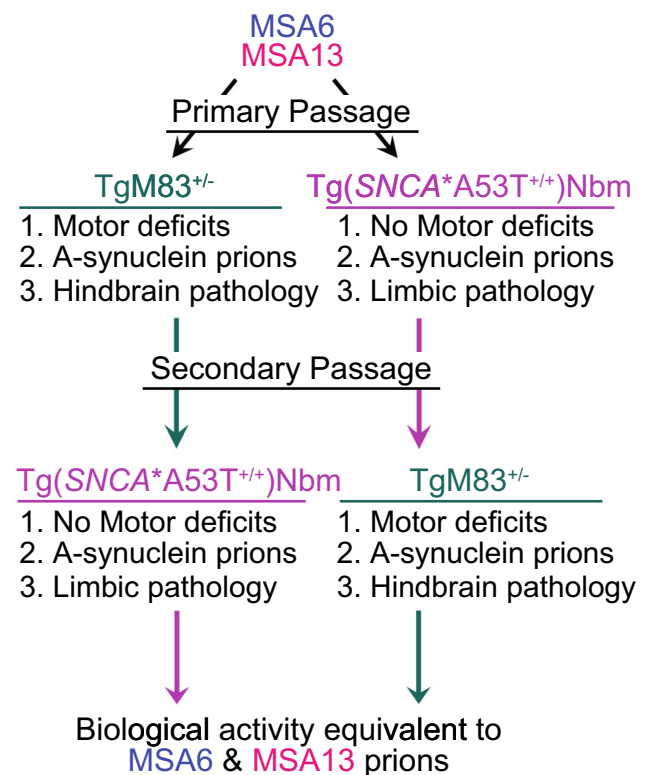

MSA6
MSA13
Primary Passage

TgM83$^{+/-}$
1. Motor deficits
2. A-synuclein prions
3. Hindbrain pathology

Tg(*SNCA**A53T$^{+/+}$)Nbm
1. No Motor deficits
2. A-synuclein prions
3. Limbic pathology

Secondary Passage

Tg(*SNCA**A53T$^{+/+}$)Nbm
1. No Motor deficits
2. A-synuclein prions
3. Limbic pathology

TgM83$^{+/-}$
1. Motor deficits
2. A-synuclein prions
3. Hindbrain pathology

Biological activity equivalent to
MSA6 & MSA13 prions

Fig. 9 Crossover studies show MSA prions can be passaged between two Tg(*SNCA**A53T) mouse models. Schematic showing the primary and secondary inoculations of MSA patient samples in TgM83$^{+/-}$ and Tg(*SNCA**A53T$^{+/+}$)Nbm mice. Patient samples MSA6 and MSA13 were first inoculated into either TgM83$^{+/-}$ or Tg(*SNCA**A53T$^{+/+}$) Nbm mice. TgM83$^{+/-}$ mice developed motor deficits, and their brains contained neuronal α-synuclein prions that accumulated throughout the hindbrain. Tg(*SNCA**A53T$^{+/+}$)Nbm mice did not exhibit motor deficits, but their brains did contain α-synuclein prions that formed inclusions in multiple cell types throughout the limbic system. Secondary passaging with these brain homogenates across the two Tg mouse models showed that TgM83$^{+/-}$ mice still developed motor deficits, α-synuclein prions, and neuronal hindbrain pathology, whereas Tg(*SNCA**A53T$^{+/+}$)Nbm mice remained asymptomatic, developed α-synuclein prions, and exhibited limbic pathology. Alpha-synuclein prions isolated from the Tg mouse models after the primary and secondary passages retained the same biological activity as the α-synuclein prions in MSA6 and MSA13 patient samples

the Tg(*SNCA**A53T$^{+/+}$)Nbm mice, but not in the other two Tg(*SNCA*)Nbm lines. Mice containing MSA prions developed phosphorylated α-synuclein inclusions mainly in neurons and astrocytes throughout the limbic system. Additionally, the α-synuclein aggregates in these mice retained biological and biochemical characteristics of α-synuclein in MSA patient samples [41], indicating faithful propagation of MSA prions in vivo.

Intriguingly, *SNCA* transgene expression is lowest in Tg(*SNCA**A53T$^{+/+}$)Nbm mice, but it was the only line to propagate MSA prions. This finding suggests that the A53T mutation disfavors the native conformation of α-synuclein

[27], stabilizes the misfolded conformation in MSA, or reduces the energy barrier between the two. Three groups have recently used cryo-electron microscopy (cryo-EM) to solve the structure of recombinant α-synuclein fibrils, and all three identified a pair of protofilaments forming a steric zipper involving the alanine at residue 53 [9, 19, 20]. In addition to this "rod polymorph," a second paired proto-filament (the "twister polymorph") assigned the R group of residue 53 to the exposed surface of the protein where it does not appear to contribute to the protofilament structure [19]. Analysis of both conformations by Li et al. showed that the A53T mutation destabilizes the steric zipper in the rod polymorph, whereas the same mutation has little impact on the energy requirements for the twister polymorph. The ability of MSA patient samples to propagate in mice expressing *SNCA**A53T argues that α-synuclein does not misfold into the rod polymorph in MSA patients. However, it is not clear from our data whether or not MSA arises from α-synuclein misfolding into the twister conformation or another, still undiscovered, conformation.

Transmission of MSA to a second Tg(*SNCA**A53T) mouse model provides additional support for the hypothesis that MSA is caused by α-synuclein prions. In MSA-inoculated TgM83$^{+/-}$ mice, neurological disease is thought to arise from the neuropathological accumulation of α-synuclein prions in the hindbrain where they disrupt autonomic and motor function. Perplexingly, we detected α-synuclein prions in MSA-inoculated Tg(*SNCA**A53T$^{+/+}$) Nbm mice in the absence of gross neurological signs. This discrepancy was explained when immunostaining of phosphorylated α-synuclein inclusions in the animals revealed that the hindbrain is unaffected by MSA prions. Instead, α-synuclein aggregates were widespread in the hippocampus and fimbria, piriform cortex and amygdala, and parahippocampal cortex. Inclusions in these brain regions would not be expected to induce autonomic or motor deficits.

Transgene expression in TgM83$^{+/-}$ mice is driven by the prion protein promoter [5], resulting in neuronal *SNCA**A53T expression and, consequentially, neuronal pathology in mice inoculated with MSA patient samples. Alternatively, the Tg(*SNCA*)Nbm lines were established using a P1 artificial chromosome, which contains the full human *SNCA* gene, its normal intron and exon structure, and 35 kb of upstream regulatory elements, meaning transgene expression is not limited to a single cell type or the CNS [17]. Previous studies using Tg(*SNCA*$^{+/+}$)Nbm mice found MSA-induced α-synuclein aggregates were predominantly localized to neurons, with occasional inclusions seen in astrocytes or microglia [1]. This is similar to our observation that α-synuclein inclusions in MSA-inoculated Tg(*SNCA**A53T$^{+/+}$)Nbm mice primarily co-localize with neurons and astrocytes, with infrequent aggregates seen in microglia and oligodendrocytes.

The work reported here is the first demonstration that MSA prions can be transmitted between two Tg mouse models. Notably, the biological and biochemical characteristics of the α-synuclein prions that cause MSA were retained after primary passaging in both the TgM83$^{+/-}$ [41] and Tg(*SNCA**A53T$^{+/+}$)Nbm animals. Based on these observations, we proposed that the α-synuclein prions in MSA-inoculated Tg(*SNCA**A53T$^{+/+}$)Nbm mice would transmit neurological disease to TgM83$^{+/-}$ mice. We investigated this hypothesis using a crossover experiment in which two MSA patient samples and one control sample were first passaged in either TgM83$^{+/-}$ or Tg(*SNCA**A53T$^{+/+}$)Nbm mice (Fig. 9). Brain homogenates from those mice were subsequently used as inoculum in secondary passage experiments between the two Tg mouse models. Serial passaging with the control patient sample had no effect in either *SNCA**A53T mouse line, indicating that the crossover inoculations alone were not responsible for inducing α-synuclein prion formation. Remarkably, we found that MSA prions first passaged in Tg(*SNCA**A53T$^{+/+}$)Nbm mice transmitted neurological disease to TgM83$^{+/-}$ animals, and we could quantify α-synuclein prions in brain homogenates from the symptomatic mice using the α-syn140*A53T–YFP cell assay. In parallel, we found that we could also detect α-synuclein prions in Tg(*SNCA**A53T$^{+/+}$)Nbm mice 300 days after inoculating them with MSA patient samples that had first been passaged in TgM83$^{+/-}$ mice. Despite the unequivocal neuropathological differences between TgM83$^{+/-}$ and Tg(*SNCA**A53T$^{+/+}$)Nbm mice after both primary and secondary passaging studies (both cell type(s) and brain regions affected), the α-synuclein prions transmitted between the two models remained unchanged from the initial MSA prions inoculated. Consistent with recent cryo-EM data, this finding argues that the conformation of the misfolded protein (rather than cellular milieu [30], mouse strain, or varied transgene expression) is responsible for determining the α-synuclein prion strain present in MSA patients. Altogether, these observations provide increasing evidence to support the hypothesis that MSA is a prion disease.

Center is supported by the National Institutes of Health (AG005134), and the Neurodegenerative Disease Brain Bank at the University of California, San Francisco, receives funding support from NIH grants P01AG019724 and P50AG023501, the Consortium for Frontotemporal Dementia Research, and the Tau Consortium.

Compliance with ethical standards

References

1. Bernis ME, Babila JT, Breid S, Wüsten KA, Wüllner U, Tamgüney G (2015) Prion-like propagation of human brain-derived alpha-synuclein in transgenic mice expressing human wild-type alpha-synuclein. Acta Neuropathol Commun 3:75

2. Carlson GA, Kingsbury DT, Goodman PA, Coleman S, Marshall ST, DeArmond S et al (1986) Linkage of prion protein and scrapie incubation time genes. Cell 46:503–511

3. Dimou L, Simon C, Kirchhoff F, Takebayashi H, Gotz M (2008) Progeny of Olig2-expressing progenitors in the gray and white matter of the adult mouse cerebral cortex. J Neurosci 28:10434–10442

4. Fleming SM, Salcedo J, Fernagut P-O, Rockenstein E, Masliah E, Levine MS et al (2004) Early and progressive sensorimotor anomalies in mice overexpressing wild-type human α-synuclein. J Neurosci 24:9434–9440

5. Giasson BI, Duda JE, Quinn SM, Zhang B, Trojanowski JQ, Lee VM (2002) Neuronal α-synucleinopathy with severe movement disorder in mice expressing A53T human α-synuclein. Neuron 34:521–533

6. Gispert S, Del Turco D, Garrett L, Chen A, Bernard DJ, Hamm-Clement J et al (2003) Transgenic mice expressing mutant A53T human alpha-synuclein show neuronal dysfunction in the absence of aggregate formation. Mol Cell Neurosci 24:419–429

7. Gomez-Isla T, Irizarry MC, Mariash A, Cheung B, Soto O, Schrump S et al (2003) Motor dysfunction and gliosis with preserved dopaminergic markers in human α-synuclein A30P transgenic mice. Neurobiol Aging 24:245–258

8. Graham JG, Oppenheimer DR (1969) Orthostatic hypotension and nicotine sensitivity in a case of multiple system atrophy. J Neurol Neurosurg Psychiatry 32:28–34

9. Guerrero-Ferreira R, Taylor NM, Mona D, Ringler P, Lauer ME, Riek R et al (2018) Cryo-EM structure of alpha-synuclein fibrils. eLife 7:e36402

10. Huang W, Zhao N, Bai X, Karram K, Trotter J, Goebbels S et al (2014) Novel NG2-CreERT2 knock-in mice demonstrate heterogeneous differentiation potential of NG2 glia during development. Glia 62:896–913

11. Ikeda M, Kawarabayashi T, Harigaya Y, Sasaki A, Yamada S, Matsubara E et al (2009) Motor impairment and aberrant production of neurochemicals in human α-synuclein A30P + A53T transgenic mice with α-synuclein pathology. Brain Res 1250:232–241

12. Jellinger KA, Lantos PL (2010) Papp-Lantos inclusions and the pathogenesis of multiple system atrophy: an update. Acta Neuropathol 119:657–667

13. Kahle PJ, Neumann M, Ozmen L, Muller V, Jacobsen H, Schindzielorz A et al (2000) Subcellular localization of wild-type and Parkinson's disease-associated mutant α-synuclein in human and transgenic mouse brain. J Neurosci 20:6365–6373

14. Kahle PJ, Neumann M, Ozmen L, Müller V, Jacobsen H, Spooren W et al (2002) Hyperphosphorylation and insolubility of alpha-synuclein in transgenic mouse oligodendrocytes. EMBO Rep 3:583–588

15. Kaji S, Maki T, Kinoshita H, Uemura N, Ayaki T, Kawamoto Y et al (2018) Pathological endogenous α-synuclein accumulation in oligodendrocyte precursor cells potentially induces inclusions in multiple system atrophy. Stem Cell Rep 10:356–365

16. Kang SH, Fukaya M, Yang JK, Rothstein JD, Bergles DE (2010) NG2+ CNS glial progenitors remain committed to the oligodendrocyte lineage in postnatal life and following neurodegeneration. Neuron 68:668–681

17. Kuo YM, Li Z, Jiao Y, Gaborit N, Pani AK, Orrison BM et al (2010) Extensive enteric nervous system abnormalities in mice transgenic for artificial chromosomes containing Parkinson disease-associated alpha-synuclein gene mutations precede central nervous system changes. Hum Mol Genet 19:1633–1650

18. Lee MK, Stirling W, Xu Y, Xu X, Qui D, Mandir AS et al (2002) Human α-synuclein-harboring familial Parkinson's disease-linked Ala-53 → Thr mutation causes neurodegenerative disease with α-synuclein aggregation in transgenic mice. Proc Natl Acad Sci USA 99:8968–8973

19. Li B, Ge P, Murray KA, Sheth P, Zhang M, Nair G et al (2018) Cryo-EM of full-length α-synuclein reveals fibril polymorphs with a common structural kernel. Nat Commun 9:3609

20. Li Y, Zhao C, Luo F, Liu Z, Gui X, Luo Z et al (2018) Amyloid fibril structure of α-synuclein determined by cryo-electron microscopy. Cell Res 28:897–903

21. Liu P, Wang X, Gao N, Zhu H, Dai X, Xu Y et al (2010) G protein-coupled receptor kinase 5, overexpressed in the α-synuclein up-regulation model of Parkinson's disease, regulates bcl-2 expression. Brain Res 1307:134–141

22. Mandler M, Valera E, Rockenstein E, Mante M, Weninger H, Patrick C et al (2015) Active immunization against alpha-synuclein ameliorates the degenerative pathology and prevents demyelination in a model of multiple system atrophy. Mol Neurodegener 10:10

23. Masliah E, Rockenstein E, Veinbergs I, Mallory M, Hashimoto M, Takeda A et al (2000) Dopaminergic loss and inclusion body formation in a-synuclein mice: implications for neurodegenerative disorders. Science 287:1265–1269

24. May VEL, Ettle B, Poehler A-M, Nuber S, Ubhi K, Rockenstein E et al (2014) α-Synuclein impairs oligodendrocyte progenitor maturation in multiple system atrophy. Neurobiol Aging 35:2357–2368

25. Nishie M, Mori F, Yoshimoto M, Takahashi H, Wakabayashi K (2004) A quantitative investigation of neuronal cytoplasmic and intranuclear inclusions in the pontine and inferior olivary nuclei in multiple system atrophy. Neuropathol Appl Neurobiol 30:546–554

26. Nishiyama A, Suzuki R, Zhu X (2014) NG2 cells (polydendrocytes) in brain physiology and repair. Front Neurosci 8:133

27. Nuber S, Rajsombath M, Minakaki G, Winkler J, Müller CP, Ericsson M et al (2018) Abrogating native α-synuclein tetramers in mice causes a L-DOPA-responsive motor syndrome closely resembling Parkinson's disease. Neuron 100:75–90

28. Papp MI, Kahn JE, Lantos PL (1989) Glial cytoplasmic inclusions in the CNS of patients with multiple system atrophy (striatonigral

degeneration, olivopontocerebellar atrophy and Shy–Drager syndrome). J Neurol Sci 94:79–100

29. Papp MI, Lantos PL (1992) Accumulation of tubular structures in oligodendroglial and neuronal cells as the basic alteration in multiple system atrophy. J Neurol Sci 107:172–182

30. Peng C, Gathagan RJ, Covell DJ, Medellin C, Stieber A, Robinson JL et al (2018) Cellular milieu imparts distinct pathological α-synuclein strains in α-synucleinopathies. Nature 557:558–563

31. Prusiner SB, Woerman AL, Mordes DA, Watts JC, Rampersaud R, Berry DB et al (2015) Evidence for α-synuclein prions causing multiple system atrophy in humans with parkinsonism. Proc Natl Acad Sci USA 112:E5308–E5317

32. Rivers LE, Young KM, Rizzi M, Jamen F, Psachoulia K, Wade A et al (2008) PDGFRA/NG2 glia generate myelinating oligodendrocytes and piriform projection neurons in adult mice. Nat Neurosci 11:1392–1401

33. Rockenstein E, Mallory M, Hashimoto M, Song D, Shults CW, Lang I et al (2002) Differential neuropathological alterations in transgenic mice expressing α-synuclein from the platelet-derived growth factor and Thy-1 promoters. J Neurosci Res 68:568–578

34. Safar J, Wille H, Itri V, Groth D, Serban H, Torchia M et al (1998) Eight prion strains have PrP^Sc molecules with different conformations. Nat Med 4:1157–1165

35. Sharon R, Bar-Joseph I, Mirick GE, Serhan CN, Selkoe DJ (2003) Altered fatty acid composition of dopaminergic neurons expressing α-synuclein and human brains with α-synucleinopathies. J Biol Chem 278:49874–49881

36. Shults CW, Rockenstein E, Crews L, Adame A, Mante M, Larrea G et al (2005) Neurological and neurodegenerative alterations in a transgenic mouse model expressing human α-synuclein under oligodendrocyte promoter: implications for multiple system atrophy. J Neurosci 25:10689–10699

37. Spillantini MG, Bird TD, Ghetti B (1998) Frontotemporal dementia and parkinsonism linked to chromosome 17: a new group of tauopathies. Brain Pathol 8:387–402

38. van der Putten H, Wiederhold K-H, Probst A, Barbieri S, Mistl C, Danner S et al (2000) Neuropathology in mice expressing human α-synuclein. J Neurosci 20:6021–6029

39. Wakabayashi K, Yoshimoto M, Tsuji S, Takahashi H (1998) α-Synuclein immunoreactivity in glial cytoplasmic inclusions in multiple system atrophy. Neurosci Lett 249:180–182

40. Watts JC, Giles K, Oehler A, Middleton L, Dexter DT, Gentleman SM et al (2013) Transmission of multiple system atrophy prions to transgenic mice. Proc Natl Acad Sci USA 110:19555–19560

41. Woerman AL, Kazmi SA, Patel S, Aoyagi A, Oehler A, Widjaja K et al (2018) Familial Parkinson's point mutation abolishes multiple system atrophy prion replication. Proc Natl Acad Sci USA 115:409–414

42. Woerman AL, Kazmi SA, Patel S, Freyman Y, Oehler A, Aoyagi A et al (2018) MSA prions exhibit remarkable stability and resistance to inactivation. Acta Neuropathol 135:49–63

43. Woerman AL, Stöhr J, Aoyagi A, Rampersaud R, Krejciova Z, Watts JC et al (2015) Propagation of prions causing synucleinopathies in cultured cells. Proc Natl Acad Sci USA 112:E4949–E4958

44. Yazawa I, Giasson BI, Sasaki R, Zhang B, Joyce S, Uryu K et al (2005) Mouse model of multiple system atrophy α-synuclein expression in oligodendrocytes causes glial and neuronal degeneration. Neuron 45:847–859

45. Young KM, Psachoulia K, Tripathi RB, Dunn SJ, Cossell L, Attwell D et al (2013) Oligodendrocyte dynamics in the healthy adult CNS: evidence for myelin remodeling. Neuron 77:873–885

46. Zhou W, Milder JB, Freed CR (2008) Transgenic mice overexpressing tyrosine-to-cysteine mutant human alpha-synuclein: a progressive neurodegenerative model of diffuse Lewy body disease. J Biol Chem 283:9863–9870

47. Zhu X, Bergles DE, Nishiyama A (2008) NG2 cells generate both oligodendrocytes and gray matter astrocytes. Development 135:145–157

48. Zhu X, Hill RA, Dietrich D, Komitova M, Suzuki R, Nishiyama A (2011) Age-dependent fate and lineage restriction of single NG2 cells. Development 138:745–753

Affiliations

Amanda L. Woerman[1,2] · Abby Oehler[1] · Sabeen A. Kazmi[1] · Jisoo Lee[1] · Glenda M. Halliday[3,4,5] · Lefkos T. Middleton[6] · Steve M. Gentleman[7] · Daniel A. Mordes[8] · Salvatore Spina[2] · Lea T. Grinberg[2] · Steven H. Olson[1,2] · Stanley B. Prusiner[1,2,9] 🅸🅳

[1] Institute for Neurodegenerative Diseases, Weill Institute for Neurosciences, University of California, San Francisco, CA, USA

[2] Department of Neurology, University of California, San Francisco, CA, USA

[3] Brain and Mind Centre, Sydney Medical School, The University of Sydney, Sydney, Australia

[4] School of Medical Science, Faculty of Medicine, University of New South Wales, Sydney, Australia

[5] Neuroscience Research Australia, Randwick, Australia

[6] Ageing Epidemiology Research, School of Public Health, Imperial College London, London, UK

[7] Division of Brain Sciences, Department of Medicine, Imperial College London, London, UK

[8] C.S. Kubik Laboratory for Neuropathology, Department of Pathology, Massachusetts General Hospital, Boston, MA, USA

[9] Department of Biochemistry and Biophysics, University of California, San Francisco, CA, USA